



OPEN ACCESS

Physiological and functional responses of water-cooled versus traditional radiofrequency ablation of peripheral nerves in rats

Christa Zachariah,¹ Jacques Mayeux,¹ Guillermo Alas,¹ Sherry Adesina,¹ Olivia Christine Mistretta,² Patricia Jill Ward,² Antonia Chen,³ Arthur William English,² Alencia V Washington¹

► Additional material is published online only. To view please visit the journal online (<http://dx.doi.org/10.1136/rpam-2020-101361>).

¹Research and Development, Avanos Medical Inc, Alpharetta, Georgia, USA

²Department of Cell Biology, Emory University, Atlanta, Georgia, USA

³Department of Orthopaedic Surgery, Brigham and Women's Hospital, Boston, Massachusetts, USA

Correspondence to

Dr Christa Zachariah, Research and Development, Avanos Medical Inc, Alpharetta, GA 30004, USA; christacaesar@gmail.com

Received 7 February 2020

Revised 8 June 2020

Accepted 29 June 2020

Published Online First

11 August 2020

ABSTRACT

Background and objectives Several clinical studies have focused on assessing the effectiveness of different radiofrequency ablation (RFA) modalities in pain management. While a direct head-to-head clinical study is needed, results from independent studies suggest that water-cooled RFA (CRFA) may result in longer lasting pain relief than traditional RFA (TRFA). The primary purpose of this study was, therefore, to investigate in a preclinical model, head-to-head differences between the two RFA technologies.

Methods RFA was performed in a rat sciatic nerve model (n=66) in two groups: (1) TRFA or (2) CRFA. The surgeon was not blinded to the treatment; however, all the physiological endpoints were assessed in a blinded fashion which include histological, MRI, and nerve function assessment via electromyography.

Results The energy delivered by the generator for CRFA was significantly higher compared with TRFA. Histological staining of nerves harvested immediately following CRFA exhibited extended length and multiple zones of thermal damage compared with TRFA-treated nerves. MRI scans across 4 weeks following treatment showed edematous/inflammatory zones present for longer times following CRFA. Finally, there was greater attenuation and prolonged loss of nerve function measured via electromyography in the CRFA group.

Conclusions This study shows that CRFA has greater energy output, as well as more pronounced structural and functional changes elicited on the peripheral nerves compared with TRFA. While these preclinical data will need to be confirmed with a large clinical randomized controlled trial, we are encouraged by the direction that they may have set for those trials.

INTRODUCTION

Radiofrequency ablation (RFA) technologies such as water-cooled RFA (CRFA)^{1,2} and traditional RFA (TRFA) offer precise, opioid-free and long-term solutions for several chronic pain conditions. RFA is minimally invasive and works by interrupting conduction through sensory neurons associated with chronic pain.^{2,3} CRFA and TRFA both use a continuous high frequency alternating current to induce ionic heating and resultant coagulative necrosis of axons in target nerves. This specific region of coagulative necrosis is also commonly referred to as a lesion.

The lesion generated from TRFA is ellipsoid in shape, with the long axis along the active tip of the probe.^{2,3} To maximize lesion effectiveness, the TRF probe is typically placed parallel to the target nerve.^{2,3} A potential drawback of parallel placement of the TRF probe tip is that lesioning sometimes occurs on only one side of the target nerve.^{2,3} As a result, the amount and duration of pain-relief achieved may be reduced and result in an early recurrence of pain. Moreover, physicians must ensure that tissue temperatures surrounding the TRF probe tip do not exceed 90°C–100°C at which point tissue dehydration occurs, causing desiccation. This, in turn, limits ionic heating resulting in unsuccessful ablations.^{2,4}

CRFA overcomes several of these limitations associated with TRFA. The active water cooling of the CRF probe tip prevents it from attaining excessively high tissue temperatures with associated tissue desiccation, thereby allowing for the continuous flow of radiofrequency (RF) energy (ionic heating) to create larger thermal and spherical lesions.⁴ This effect allows for the probe to be placed on target tissues independent of orientation relative to the nerve and provides a larger distal projection.² There are newer TRF probe designs that are available that have protruding electrodes that generate larger lesions than TRF probes, however, ex vivo studies show that lesion volumes of these protruding probes are smaller by more than 50% compared with the volumes generated by CRF probes⁵ and do not allow for angle independence or provide larger distal projections.

Clinical studies assessing knee pain outcomes following genicular nerve RFA report pain relief lasting for 3–6 months for TRFA^{6–10} and 6–12 months or even longer for CRFA.^{11–15} A possible hypothesis for the clinically observed prolonged pain relief following CRF ablations^{11–13} is that the lesions generated by this modality damage sensory nerves to a greater degree—both structurally and functionally. However, this hypothesis has not been tested in vivo or in robust, randomized clinical studies. Furthermore, RF lesions have been primarily evaluated only for size and volume in non-vascularized, ex vivo tissue models (such as the chicken-breast, bovine liver or tissue phantoms).^{5,16,17} A thorough characterization of the physiological changes in response to either TRFA or CRFA in a survival animal model is lacking. The



© American Society of Regional Anesthesia & Pain Medicine 2020. Re-use permitted under CC BY-NC. No commercial re-use. Published by BMJ.

To cite: Zachariah C, Mayeux J, Alas G, et al. *Reg Anesth Pain Med* 2020;**45**:792–798.

primary goal of this study, therefore, was to evaluate the immediate and physiological effects of CRFA and TRFA, and to relate the structural changes following ablation to functional outcomes in a survival, *in vivo* model. It was hypothesized that the higher energy used for CRFA leads to a larger, longer lasting lesion resulting in the loss of nerve function to a greater magnitude and prolonged duration in comparison to TRFA.

METHODS

Animals

Male Lewis rats, between the ages of 10–12 weeks, and between 250 and 300 g were used in all studies. The animals were kept on a 12-hour light/dark schedule and had unlimited access to food and water.

Animals were anesthetized either using 1%–2% isoflurane or a combination of ketamine (150 mg/kg) and xylazine (9.6 mg/kg). Buprenorphine was administered once only for postprocedural pain relief and did not complicate any subsequent analysis. A 2–3 cm skin incision was made on the posterior thigh, adjacent to the sciatic notch. Using blunt forceps, the sciatic nerve (SN) was exposed by carefully separating surrounding connective tissue and hamstring muscles. Following this, either a TRFA cannula (22-gauge, 100 mm long, 5 mm active tip—PMF-22-100-5; Avanos Medical, Alpharetta, Georgia, USA) or CRFA introducer (17-gauge, 75 mm long, 2 mm active tip—CRI-17-75-2; Avanos Medical) was introduced through the skin just distal to the exposed nerve, under direct vision. The stylet was then removed and the respective probe (PMP-22-100-5, TRFA and CRP-17-75-2, CRFA, Avanos Medical) was positioned directly under the SN (parallel placement for TRFA and angle independent placement for CRFA). These probe sizes were chosen to replicate previously published rodent ablation survival studies by Choi *et al*¹⁸ and to minimize adverse events that might result from use of larger probes. A bolus of saline was added directly over the exposed SN to moisten the tissue and improve electrode-nerve contact. An impedance measurement was then taken from the generator (PMG-Advanced, Avanos Medical) and if the values

fell within the expected range (150–200 Ω), the RF generator was initiated in auto-temp mode to start the ablation. Note that the nerve was not exposed to air at the time of ablation.

The placement of the probe and the distribution of the animals into the various study groups may be referred to in figure 1. In the first cohort of animals (n=11 per group), the RF procedure parameters were set to what is currently used in the clinical setting. For the TRFA group, the RF current was delivered at a set temperature of 80°C for 90 seconds (s), while the RF current for the CRFA group was delivered at a set temperature of 60°C for 150 s. The animals in this cohort (total of 22) were euthanized within 2 hours on the same day following the ablation and nerves harvested for histological assessment in a blinded fashion.

In the second cohort of animals (n=12 per RF group), the RF current for both groups was delivered at a lower run duration to allow for their survival over several weeks (12 weeks) without adverse events (toe chewing, foot swelling and heel scabs) and to maintain a similar ratio in total energy delivered as is observed using clinical run parameters for both treatment groups. The RF current was delivered at 80°C for 50 s for the TRFA group or at 60°C for 80 s for the CRFA group. A third group of animals (n=6) in the second cohort received a transection of the SN wherein the nerve was cut and repaired by end-to-end anastomosis, securing the repair with fibrin glue as previously described.¹⁹ This group served as a positive control. A surgical sham group (n=6) was also included in the second cohort wherein the SN was exposed, and the probe was placed, but these animals did not receive an ablation.

For both cohorts, the subcutaneous surgical site was closed using buried sutures and skin was closed using staples. Following this, a small amount of topical analgesic was applied to the external surgical site.

Power output recording and energy calculations

During the ablation procedure, a laptop connected to the generator recorded the power output every 0.2 s. Following the procedures, the total energy delivered by the generator was calculated

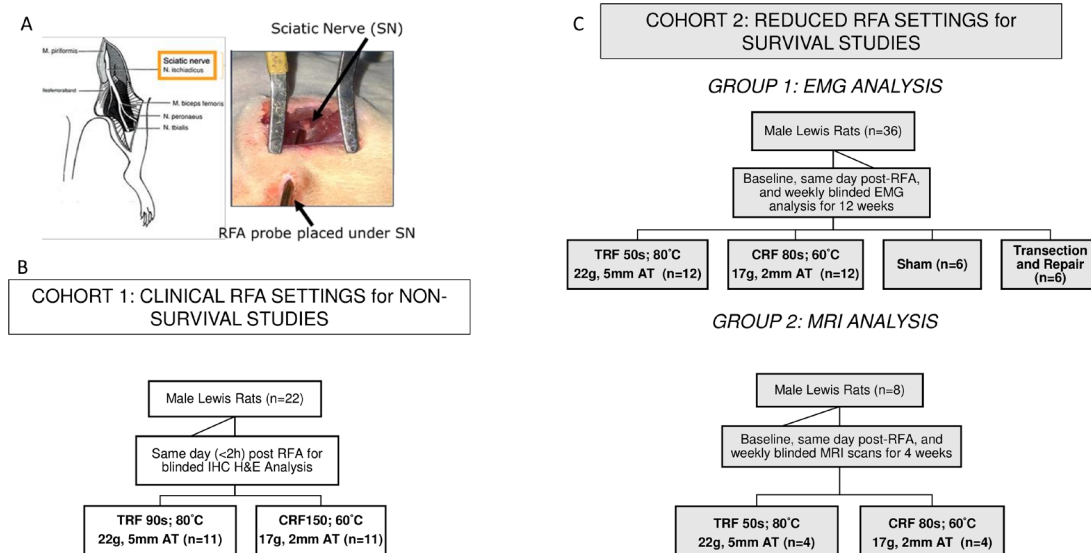


Figure 1 Probe placement and Study Design. (A) The probe tip was placed directly under the sciatic nerve (parallel placement for TRF and angle independent for CRF) using visual guidance. (B) Cohort 1 included rats that were distributed into two treatment groups for same-day immunohistochemistry (IHC) analysis, using clinical run parameters (C) Cohort 2 included a group of rats that were survived for 12 weeks for EMG analysis and another group that was survived for 4 weeks for MRI analysis. CRF, cooled radiofrequency; EMG, electromyography; RFA, radiofrequency ablation; TRF, traditional radiofrequency.

for every TRFA or CRFA run. The total energy (in Joules, J) delivered by the RF generator was quantified by integrating the total power delivered across the total run duration, for varying RF ablation run times typically used in the clinic (>80 s).

Histological analyses

For the first cohort of animals, to quantify the initial injury induced in vivo by both CRF or TRF ablations, SNs were collected within an hour following ablation. Following euthanasia via intracardiac injection of pentobarbital sodium and phenytoin sodium solution (2 mEq/kg) with isoflurane plane of anesthesia, the SNs were carefully extracted and postfixed in 10% formalin, embedded in paraffin and sectioned longitudinally (along the length of the nerve) into 5 μ m thick sections. These were then stained with H&E to assess the degree of thermal damage to the local and surrounding cell and tissue structures. An independent histopathologist (Histotox Labs, Boulder, Colorado, USA) then assessed and measured the degree of thermal damage in all samples. H&E-stained step slides (five levels per sample) were scanned and lesion measurements were performed on whole slide images. The total length of the lesioned areas (lesion extent) captured on each slide was measured (in mm). The ablation zone was defined as the entire region of coagulated collagen and/or acute necrosis (including a central cooled zone, if present); collagen coagulation was characterized by swelling, altered morphology and increased amphophilia (purple/blue color instead of pink) of endoneurial, perineurial and/or epineurial collagen.

MRI

In a subset of the second cohort of animals, MRI scans were performed immediately following ablation (<1 hour; n=4) and once weekly for up to 4 weeks (n=4 at 1 week, 4 at 2 weeks, 4 at 3 weeks and 4 at 4 weeks) using a Bruker 9.4T scanner and the Fast Low Angle Shot (FLASH) and Rapid Acquisition with Relaxation Enhancement (RARE) MRI sequences. T1W images (FLASH): TR/TE=600/3.2 ms, FA=Avg.=4, matrix=256x256, FOV=60x60 mm², slice thickness=1 mm, number of slices=30. T2W images (RARE) TR/TE=4000/40 ms, RARE factor=4, Avg.=4, matrix=256x256, FOV=60x60 mm², slice thickness=1mm, number of slices=30. The slice locations were equivalent in T1W and T2W images. The area of hyperintensity on the MRI scans for all the slices were also quantified using the Mimics software (Materialize, Leuven, Belgium) and the total volume calculated for all the ablations.

Electromyography

In the second cohort of animals, fine wire bipolar electromyography (EMG) electrodes (California Fine Wire Company, Grover Beach, California, USA; Stablohm 800 A, material number cfw-100189) were inserted into the gastrocnemius (GAS) and tibialis anterior (TA) muscle via 25-gage hypodermic needles. Electrodes were implanted into the GAS or TA muscle in every animal to reduce variability while recording data. EMG activity was recorded from these electrodes in response to stimulation of the SN in 0.3 ms pulses. Stimulus intensity was adjusted to elicit maximal M-responses (short latency direct muscle responses) from electrical stimulation of the SN before and at different times after ablation (immediately after, and 1, 2, 4, 6, 8, 10 and 12 weeks postablation). The duration, amplitude and latency of these maximal M-responses were measured from the evoked responses, as described in our earlier work.²⁰

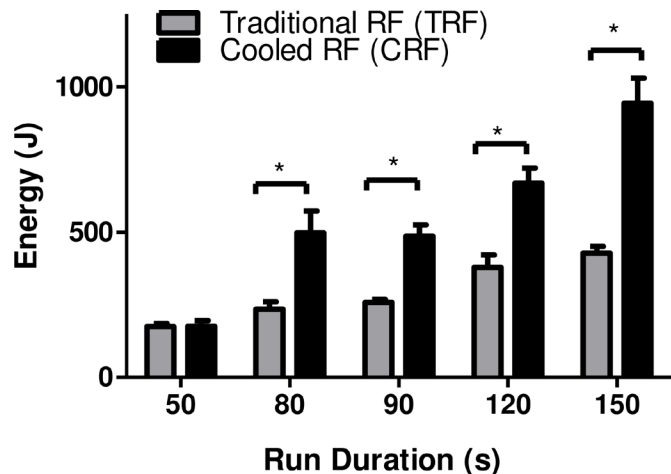


Figure 2 Cooled RF ablations use more energy than traditional RF at >60 s run durations. The energy (in joules, J) used to generate a TRF or CRF ablation was calculated at 50 seconds (s), 80 s, 90 s, 120 s or 150 s. CRF ablation uses more energy at all time points >60 s (80 s, 90 s, 120 s or 150 s) to generate the thermal lesion at the nerve. Bars represent mean \pm SD. *P<0.05 for n=3–13 per group per timepoint. RF, radiofrequency.

Statistical analysis

All quantitative data are expressed as mean \pm SD or SE mean and are noted as such under each figure. Statistical analysis was performed on GraphPad Prism V.5.0 statistical software (Graphpad Software, La Jolla, California, USA) using either a two-tailed Student's t-test to compare mean values obtained from two groups, or a one-way or two-way analysis of variance (ANOVA) to compare the means of multiple treatment groups. Post hoc tests for multiple comparisons were used where appropriate. Statistical significance was set at p<0.05.

RESULTS

More energy is delivered by the RF generator for CRFA lesions than TRFA lesions

The energy delivered at the time of each ablation performed was measured from the RF generator. The mean (\pm SD) energy delivered at different run durations for CRFA and TRFA is shown in [figure 2](#). The RF generator delivered significantly more energy during a CRFA compared with the corresponding TRFA (CRFA vs TRFA: 943.4 \pm 311 J vs 427.8 \pm 49.8 J at 150 s; 667.7 \pm 117.3 J vs 378.9 \pm 94.3 J at 120 s, 485.5 \pm 67.6 J vs 257.7 \pm 36.2 J at 90 s, and 497.8 \pm 183.7 vs 235.1 \pm 54.6 J at 80 s). A two-way ANOVA compared the five groups. If the results of this ANOVA were positive (p<0.05), paired post hoc tests (Tukey) were performed to evaluate intragroup or intergroup significance of differences.

CRF ablations produce larger lesions in vivo that persist for longer than traditional RF lesions

Histological assessment of initial RF injury

SNs were harvested immediately after ablation and prepared for histological analysis. Representative longitudinal sections of ablated nerves are shown in [figure 3](#). SNs treated with CRFA for 150 s were observed to have longer lesion lengths ([figure 3A](#), quantified in [figure 3B](#)) compared with those that were ablated for 90 s with TRFA using an unpaired t-test ([figure 3A](#), quantified in [figure 3B](#)). In 9 of the 11 CRFA treated SN samples (representative images shown in [figure 3A](#)), the ablation zone following H&E staining showed regions of lesser damage (lighter purple

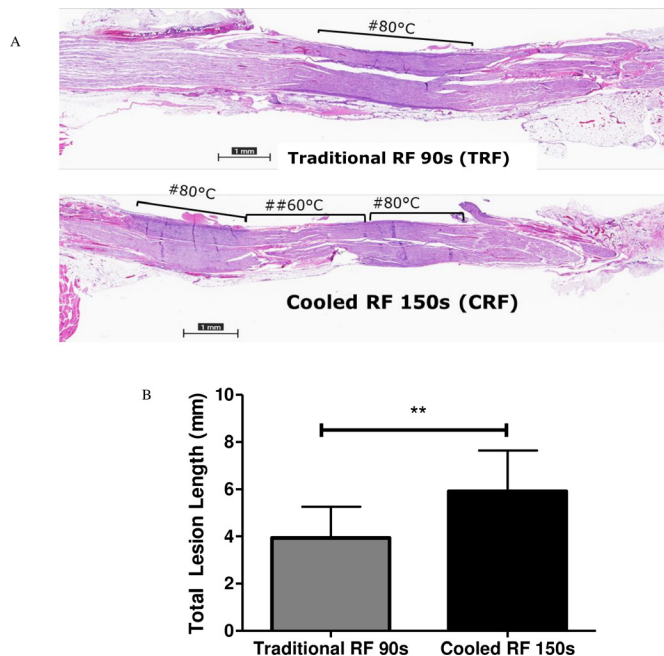


Figure 3 Longer lesions with three distinct zones of thermal damage (dark pink or purple zones) which correspond to the predicted 60°C and 80°C thermal profile was observed in CRF treated nerves. (A) Representative H&E-stained longitudinal, sciatic nerve sections following TRF treatment (above) and CRF treatment (below) (n=9–11) #regions corresponding to 80°C thermal damage (purple); ##regions corresponding to 60°C thermal damage (dark pink). (B) Lesion lengths for both treatment groups were measured by a histopathologist who was blinded to the treatment groups. CRF lesion lengths were significantly longer than TRF treated groups. Bars represent mean±SD; **p<0.01, n=9 for the CRF group and n=11 for the TRF group. RF, radiofrequency.

stain) flanked by two regions of more severe damage (purple stain). On the other hand, there was only a single zone of thermal damage (purple stain) observed in the TRFA treated SNs (representative example shown in [figure 3B](#)). The average total length of the ablation zone was significantly greater in CRF samples (5.924 ± 1.7 mm) than TRFA treated samples (3.935 ± 1.3 mm).

MR analysis of the RF-induced lesion sites

To assess the structural changes at the lesion zone following ablations, T2-weighted MRI images of the ablated rats immediately after (<1 hour) and weekly (for up to 4 weeks) postablation using a 9.4T Bruker scanner was acquired in the second cohort of rats. Representative images through the ablation sites are shown in [figure 4A](#). Distinct inflammatory and edematous ‘lesion zones’ (indicated by yellow arrows in [figure 4](#)) were observed in the tissue areas surrounding the SN ablated by both treatment groups immediately after ablation. These ‘lesion zones’ were present in both groups at 1 week following ablation. At week 2, they are almost imperceptible in the TRFA group but are still present in the CRFA group. The lesion volumes were calculated using the Mimics Software tool and the mean volumes are presented in [figure 4B](#). The volume of the ‘lesion zone’ immediately following the ablation was significantly higher in the CRFA group (1169 ± 271.9 mm³) compared with the TRFA group (775.9 ± 240.3 mm³). An unpaired t-test was used to evaluate the significance of difference between the two treatments at each time point.

Electrical conduction in axons in the SN is interrupted for longer times after CRF ablation than TRF ablation

Evoked electrical activity of the GAS and TA muscles, which are innervated by the SN, was measured as an indicator of conduction along motor axons, prior to, immediately after, 1 week, 2 weeks and then biweekly for up to 12 weeks postablation. Mean amplitudes of direct muscle responses (M-responses) were significantly reduced from baseline in both GAS and TA in TRFA and CRFA animals, as well as in rats in which the SN had been cut and repaired, at 1-week postablation ([figure 5A,B](#)). However, as early as 1 week following ablation and for the subsequent 6 weeks, evoked M-response intensity was significantly smaller in the CRFA group and the transection and repair group than in animals exposed to TRFA ([figure 5A,B](#)). A similar effect was found in both the GAS and TA muscles. The degree of reduction in M-response amplitude found in the CRFA treated group was comparable to that observed in the transected nerve injury group at the 1, 2, 4 and 6 weeks time points ([figure 5A,B](#)). Nerve conduction recovered eventually for all groups by week 12. A one-way ANOVA compared the three groups. If the results of this ANOVA were positive (p<0.05), paired post hoc tests (Tukey) were performed to evaluate significance of differences between groups.

DISCUSSION

The underlying hypothesis for this study was that the increased energy delivered during a CRFA creates an enhanced lesion on the target nerve, resulting in prolonged loss and delayed recovery of nerve function. The findings of this study are threefold. First, the energy delivered by the generator to create CRFA is greater compared with TRF ablations, for all run times exceeding sixty seconds. Second, using the histological findings presented, we show extended zones of thermal damage along the nerve in CRF-treated SNs and corroborate previous ex vivo studies showing that CRFA generated larger lesions.⁵ Lastly, we demonstrate that CRFA effectively blocks nerve function for a longer duration and to a larger degree, compared with TRFA.

There are no known survival in vivo animal studies that have assessed the effects of CRFA on peripheral nerves across several weeks, and there are only a handful that have used the rat model to explore the effects of pulsed RFA or TRFA on peripheral nerves in a survival model.^{18–21} There are, however, several studies that have successfully used the rat SN model to explore peripheral nerve damage, neuropathic pain and nerve repair^{20–22} with clinically relevant implications. For these reasons, we chose the rat SN ablation model. There are several other advantages the rat SN model offered. The rat SN is comparable in size to the sensory nerves typically targeted for knee ablations in the clinic²³ and this allowed for the use of pain medicine equipment currently used in the clinic. Additionally, the SN is a mixed nerve containing both motor and sensory neurons, which enables quantitative assessment of nerve function by EMG.

The findings of this study have several clinically relevant implications and provide a possible explanation for the differences in pain relief observed in patients treated with varied RF ablation modalities.^{6–15} The increased energy seen in CRFA treated animals suggests that local tissues surrounding the active tip attain enhanced thermal energy,² which in turn creates a larger distal projection allowing for angle independence in probe placement for physicians.²⁴ The discovery of multiple zones of thermal damage within the CRFA lesion are novel and provide evidence for the first time in vivo of the predicted thermal profile shown previously only in ex vivo chicken breast models.⁵ In an

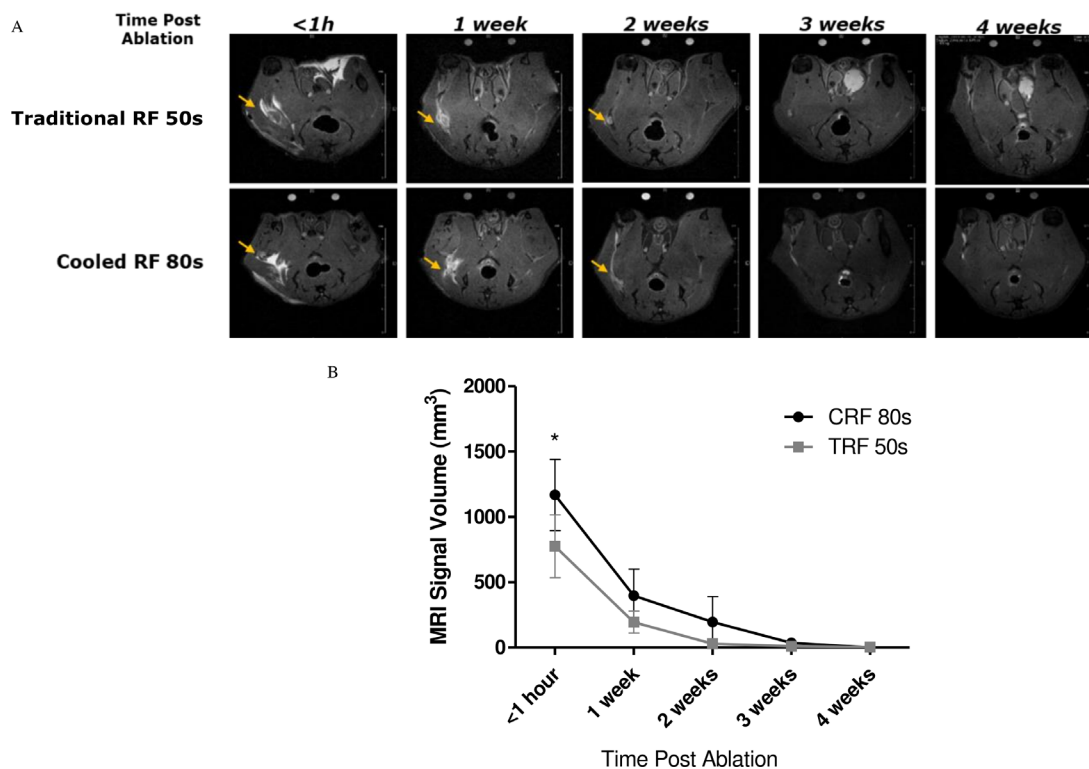


Figure 4 Distinct lesion zones ('white zones' indicated by yellow arrows in <math><1\text{-hour}</math> panels) detectable for up to 2 weeks postablation in cooled RF treatment group. (A) Representative images depict axial, T2-weighted MR scans, acquired from a 9.4T Bruker scanner. ($n=4\text{--}6$ per group per time point) (B) Quantified volumes of signal hyperintensity surrounding the lesion site at various time points using the mimics software (bars represent mean \pm SD, $n=4\text{--}6$ per group per time point; $*p<0.05$). RF, radiofrequency.

overwhelming majority of the CRFA treated nerves, a central (or 'cooled') zone of thermal damage corresponding to the temperature attained by tissues in direct contact with the 60°C probe tip is found. This 'cooled' zone is flanked by two larger zones of greater (or 'hotter') thermal damage, with levels of collagen coagulation similar to those observed in the 80°C TRFA nerve ablation zones, indicating that the tissue temperatures here also attain 80°C. It is important to note that most mammalian tissues experience irreversible thermal damage at 46°C–49°C.^{2,25} These multiple zones of CRFA-induced thermal damage indicate that

extended portions of the targeted nerve are therapeutically impacted by the CRFA probe. A report by Malik *et al* claims that prolonged pain relief following CRFA in patients may also be attributed to CRFA probes enabling the maintenance of temperatures of larger tissue volume in a narrow-desired range, allowing for additional neuromodulation of nociceptive pathways.²⁶ This additional neuromodulatory benefit following CRFA, however, should be further assessed in the future in similar animal models.

The larger lesion volume observed immediately following CRFA could be correlated with the slower resolution of the

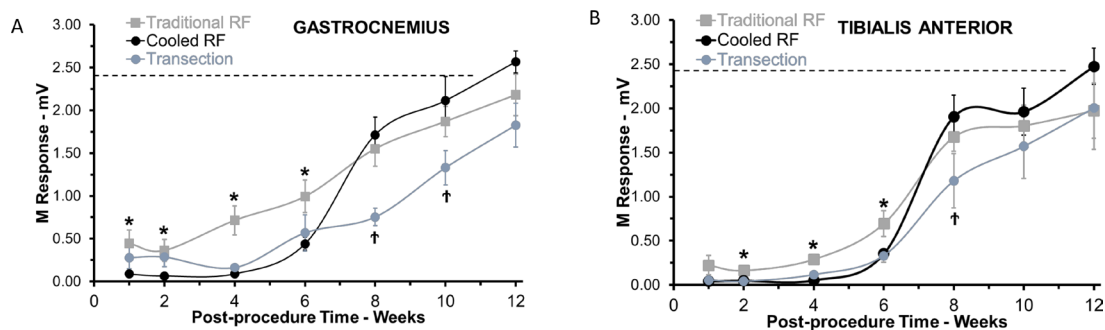


Figure 5 Recovery of electromyographic (EMG) activity following TRF ablation, CRF ablation or transection of the sciatic nerve. (A) Average gastrocnemius muscle EMG activity for 10–12 rats (per group per timepoint) during a 12-week period after ablation of the sciatic nerve using TRF (dark gray line), CRF (black line), or transection (light gray line). EMG activity is significantly reduced from pretreatment baseline (dotted line) at 1-week post-treatment in all groups. However, the CRF ablation group has significantly lower EMG activity compared with the TRF group, for up to 6 weeks postablation. Each point represents the mean \pm SEM, $*p<0.05$. (B) Average tibialis anterior (TA) muscle EMG activity for 10–12 rats (per group per timepoint) during a 12-week period after ablation of the sciatic nerve using TRF (dark gray line), CRF (black line) or transection (light gray line). EMG activity is significantly reduced from pretreatment baseline (dotted line) at 1-week post-treatment in all groups, however, even in the TA the CRF ablation group has significantly lower EMG activity compared with the TRF group for up to 6 weeks postablation. Each point represents the mean \pm SEM, $*p<0.05$. RF, radiofrequency; SEM, SE of mean.

inflammatory response, which could explain the slower attenuation of the MRI signal at week four following ablation. This also provides possible structural evidence for the observation of the longer duration of reduced nerve function in the CRFA group.

The EMG data demonstrate that as early as 1 week following treatment, SNs treated with TRFA had a larger M-response compared with CRFA or the active control (transection) group. This is potentially indicative of a fundamental difference between the two technologies. One hypothesis is that the larger M-response following TRFA may be due to a smaller proportion of motor neurons being impacted/attenuated as compared with CRFA treatment (or transection). This needs to be confirmed using techniques, such as retrograde fluorescence imaging, which would allow for both the qualitative and quantitative assessment of the motor and sensory neurons at different time points following treatment.

Additionally, it is also possible that these two RFA technologies differentially impact structures involved in nerve function (or pain perception) that extend beyond the nerve itself—such as the dorsal root ganglion (DRG). Some preliminary studies done by our group assessing differences in arrays of genes involved in inflammation and neuropathic pain signaling discovered differential expression profiles at the DRG following TRFA or CRFA. However, both these hypotheses need to be tested by well-powered studies in the future to further assess the fundamental differences between both these RFA modalities.

There are several limitations and assumptions made in this study. One particular challenge in creating a preclinical model to study clinical devices is to try and represent every clinical use case. A shortcoming of the current study is the use of only one probe size for both CRFA and TRFA, when it is known that multiple larger probe sizes for each technology may be used in the clinic. To address this issue, data from a preliminary study in the current manuscript (see online supplementary figure 6) are included in which we begin using multiple probe sizes for CRFA and TRFA. We found that even with the use of larger gage TRF probes, CRFA still delivers greater energy (up to 1.8 times more comparing the two largest probes and 3.7 times more energy comparing the smallest probes). Future studies, however, should continue to consider clinical use case in model design. Another limitation was the choice of M-responses measured from the muscle bundles innervated by the SN as an endpoint. The assumption made here was that motor axon restoration parallels sensory axon conduction and repair. EMG was selected because it was readily quantifiable and served as an excellent surrogate for sensory nerve function. Future studies should further explore sensory nerve function directly and better investigate as many aspects of the varied, complex processes involved in pain perception. These range from using a pain model, to measuring direct sensory nerve function (via paw withdrawal threshold assessment using the von Frey method, sensory nerve action potential, nociceptive flexion response), peripheral nerve repair and regeneration (via retrograde fluorescence imaging or transgenic rodent models), and peripheral and central sensitization changes in response to the varied RF treatment modalities.

The observation of prolonged pain relief following CRFA in patients led us to design an in vivo study that would better highlight physiological outcome differences between the two thermal RFA treatment modalities, and to move beyond typical ex-vivo lesion volume analyses. The rat SN ablation model was successfully developed in this study and showed reduction in nerve function post-CRFA across several weeks. The results described above provide evidence for the first time in vivo that CRFA results from the delivery of increased energy by the RF

generator which drives extended lesion zones on the target nerve. Collectively, these results provide a first glimpse at the differences in physiologic endpoints, beyond the lesion size that exist between the two thermal RF treatment modalities and the potential impact these may have on clinical outcomes.

Acknowledgements The authors acknowledge the team at 4P Labs for support with the non-survival studies and Histotox Labs (Boulder, Colorado) for their support in the histological staining and analysis of the SNs used in this study, and the Emory Center for Systems Imaging Core and Jaekeun Park, PhD for their contribution in collecting the MRI data presented here. The authors would also like to thank David Provenzano for his valuable input and insights in the design and outcomes of this study.

Contributors Each named author has substantially contributed to conducting the underlying research (planning, execution, data analysis and interpretation) and drafting of this manuscript.

Funding This study was funded by Avanos Medical Inc.

Competing interests CZ was employed by Avanos Medical as a Research Scientist. JM was employed by Avanos Medical as a Senior Research Scientist. GA is employed by Avanos Medical as a Research Scientist. SA was employed by Avanos Medical as a Research Scientist. AC reports personal fees from SLACK publishing, other from Joint Purification Systems, personal fees from Stryker, personal fees from bOne, other from Sonoran Biosciences, other from Graftworx, grants from OREF, personal fees from Pfizer, personal fees from Avanos, personal fees from Irrisep, personal fees from Convatec, personal fees from 3M, personal fees from Recro, personal fees from Heraeus, other from Hyalex, personal fees from DePuy, other from The Journal of Bone and Joint Surgery, personal fees from GLG, personal fees from UpToDate, outside the submitted work; and Editorial board: Journal of Arthroplasty; Annals of Joint; Bone and Joint 360 Journal; Clinical Orthopaedics and Related Research; Healthcare Transformation; Journal of Bone and Joint Infection; Knee Surgery, Sports Traumatology, Arthroscopy. Board / committee member: AAOS, AJRR, AAHKS, European Knee Association, International Congress for Joint Reconstruction, Musculoskeletal Infection Society. AWE reports personal fees from AVANOS Medical Science Advisory Board, outside the submitted work; AVW was employed by Avanos Medical as a Manager.

Patient consent for publication Not required.

Ethics approval All procedures were approved by 4P Labs or Emory University Institutional Animal Care and Use Committee (IACUC).

Provenance and peer review Not commissioned; externally peer reviewed.

Data availability statement Data are available on reasonable request. All data relevant to the study are included in the article or uploaded as supplementary information. Any additional information desired may be requested from corresponding author.

Open access This is an open access article distributed in accordance with the Creative Commons Attribution Non Commercial (CC BY-NC 4.0) license, which permits others to distribute, remix, adapt, build upon this work non-commercially, and license their derivative works on different terms, provided the original work is properly cited, an indication of whether changes were made, and the use is non-commercial. See: <http://creativecommons.org/licenses/by-nc/4.0/>.

REFERENCES

- Soloman M, Mekhail MN, Mekhail N. Radiofrequency treatment in chronic pain. *Expert Rev Neurother* 2010;10:469–74.
- Rea W, Kapur S, Mutagi H. Radiofrequency therapies in chronic pain. *Continuing Education in Anaesthesia Critical Care & Pain* 2011;11:35–8.
- Choi EJ, Choi YM, Jang EJ, et al. Neural ablation and regeneration in pain practice. *Korean J Pain* 2016;29:3–11.
- Wray Joseph K, Walls AL. *Radiofrequency ablation*. StatPearls, 2018.
- Cedeno DL, Vallejo A, Kelley CA, et al. Comparisons of lesion volumes and shapes produced by a radiofrequency system with a cooled, a protruding, or a monopolar probe. *Pain Physician* 2017;20:915–22.
- Choi W-J, Hwang S-J, Song J-G, Schiltenswolf M, Fischer C, et al. Radiofrequency treatment relieves chronic knee osteoarthritis pain: a double-blind randomized controlled trial. *Pain* 2011;152:481–7.
- Sari S, Aydin ON, Turan Y, et al. Which one is more effective for the clinical treatment of chronic pain in knee osteoarthritis: radiofrequency neurotomy of the genicular nerves or intra-articular injection? *Int J Rheum Dis* 2018;21:1772–8.
- Santana Pineda MM, Vanlinthout LE, Moreno Martin A, et al. Analgesic effect and functional improvement caused by radiofrequency treatment of Genicular nerves in patients with advanced osteoarthritis of the knee until 1 year following treatment. *Reg Anesth Pain Med* 2017;42:62–8.

- 9 Kirdemir P, Çatav S, Alkaya Solmaz F, Solmaz FA. The genicular nerve: radiofrequency lesion application for chronic knee pain. *Turk J Med Sci* 2017;47:268–72.
- 10 Iannaccone F, Dixon S, Kaufman A, et al. A review of long-term pain relief after Genicular nerve radiofrequency ablation in chronic knee osteoarthritis. *Pain Physician* 2017;20:E437–44.
- 11 Davis T, Loudermilk E, DePalma M, et al. Prospective, multicenter, randomized, crossover clinical trial comparing the safety and effectiveness of cooled radiofrequency ablation with corticosteroid injection in the management of knee pain from osteoarthritis. *Reg Anesth Pain Med* 2018;43:84–91.
- 12 Davis T, Loudermilk E, DePalma M, et al. Twelve-month analgesia and rescue, by cooled radiofrequency ablation treatment of osteoarthritic knee pain: results from a prospective, multicenter, randomized, cross-over trial. *Reg Anesth Pain Med* 2019;44:499–506.
- 13 Chen Aet al. *Cooled radiofrequency ablation provides 12 month durability and rescue analgesia in the management of osteoarthritic knee pain: results from a prospective, multicentered, randomized, cross-over trial*. New Orleans: American Society for Regional Anesthesia (ASRA), 2019.
- 14 Bellini M, Barbieri M. Cooled radiofrequency system relieves chronic knee osteoarthritis pain: the first case-series. *Anaesthesiol Intensive Ther* 2015;47:30–3.
- 15 Hunter C, Davis T, Loudermilk E, et al. Cooled radiofrequency ablation treatment of the Genicular nerves in the treatment of osteoarthritic knee pain: 18- and 24-month results. *Pain Pract* 2020;20:238–246.
- 16 Provenzano DA, Liebert MA, Somers DL. Increasing the NaCl concentration of the preinjected solution enhances monopolar radiofrequency lesion size. *Reg Anesth Pain Med* 2013;38:112–23.
- 17 Vallejo R, Benyamin R, Tilley DM, et al. An ex vivo comparison of cooled-radiofrequency and bipolar-radiofrequency lesion size and the effect of injected fluids. *Reg Anesth Pain Med* 2014;39:312–21.
- 18 Choi S, Choi HJ, Cheong Y, et al. Internal-Specific morphological analysis of sciatic nerve fibers in a radiofrequency-induced animal neuropathic pain model. *PLoS One* 2013;8:e73913.
- 19 Akhter ET, Rotterman TM, English AW, et al. Sciatic nerve cut and repair using fibrin glue in adult mice. *Bio Protoc* 2019;9:e3363.
- 20 Boeltz T, Ireland M, Mathis K, et al. Effects of treadmill training on functional recovery following peripheral nerve injury in rats. *J Neurophysiol* 2013;109:2645–57.
- 21 Li D-Y, Meng L, Ji N, et al. Effect of pulsed radiofrequency on rat sciatic nerve chronic constriction injury: a preliminary study. *Chin Med J* 2015;128:540–4.
- 22 Sabatier MJ, Redmon N, Schwartz G, et al. Treadmill training promotes axon regeneration in injured peripheral nerves. *Exp Neurol* 2008;211:489–93.
- 23 Manzano D, Jimenez F, Blasi M. Ultrasound-Guided pain interventions in the knee region. *Techniques in Regional Anesthesia and Pain Management* 2013;17:131–9.
- 24 Gupta A, Huettner DP, Dukewich M. Comparative effectiveness review of cooled versus pulsed radiofrequency ablation for the treatment of knee osteoarthritis: a systematic review. *Pain Physician* 2017;20:155–71.
- 25 Ball RD. The science of conventional and water-cooled monopolar lumbar radiofrequency rhizotomy: an electrical engineering point of view. *Pain Physician* 2014;17:175–211.
- 26 Malik K, Benzon HT, Walega D. Water-Cooled radiofrequency: a neuroablative or a neuromodulatory modality with broader applications? *Case Rep Anesthesiol* 2011;2011:1–3.